

Photorefractivity in Nematic Liquid Crystals Doped with a Conjugated Polymer: Mechanisms for Enhanced Charge Transport

Gary P. Wiederrecht,[†] Mark P. Niemczyk,[†]
Walter A. Svec,[†] and Michael R. Wasielewski^{*,†,‡}

Chemistry Division, Argonne National Laboratory,
Argonne, IL, 60439-4831, and
Department of Chemistry, Northwestern University,
Evanston, IL, 60208-3113

Received February 17, 1999

Revised Manuscript Received April 19, 1999

New organic materials that exhibit photorefractive effects are of wide interest for potential optical signal processing applications.^{1–13} The photorefractive effect is a light-induced change in the refractive index of a nonlinear optical material that results from the creation of a spatially periodic electric field (space-charge field). This space-charge field is produced by photoinduced charge separation within the illuminated regions of an optical interference pattern of fringe spacing, Λ , created in the material by two coherent, crossed laser beams. This is followed by charge migration of the most mobile charge carrier over micron distances into the dark regions of the interference pattern to produce a refractive index grating. Thus, optimization of the photorefractive effect in a material depends on achieving high optical nonlinearity coupled with efficient charge generation and transport.

Nematic liquid crystals reorient easily in weak electric fields and their high birefringence provides an efficient electro-optic mechanism that makes them excellent candidates for photorefractive materials.^{4–9} However, inducing efficient charge transport in these materials

is not as straightforward, and previous studies rely on photoinduced heterolytic cleavage of dye molecules or intermolecular electron transfer to create mobile anions and cations. These mobile charges obey the current density (J) equations given by^{14,15}

$$J = J^+ + J^- \quad (1)$$

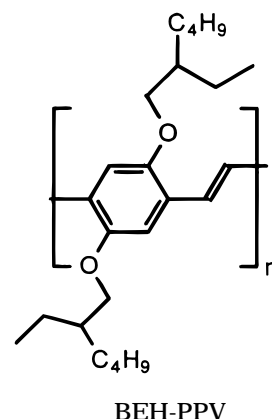
$$J^\pm = q\mu^\pm n^\pm(x,t)(E_{SC}(x,t) - E_A) \mp qD^\pm \frac{\partial n^\pm(x,t)}{\partial x} \quad (2)$$

where μ^\pm is the mobility of the cations and anions, x is the grating wavevector axis, $n^\pm(x,t)$ is the ion density, $E_{SC}(x,t)$ is the magnitude of the space-charge field, E_A is the magnitude of the applied field, q is the unit charge, and D^\pm is the diffusion constant of the cations and anions, respectively. The first term on the right-hand side of eq 2 describes charge drift, and the second term describes ion diffusion. Previous studies of photorefractivity in liquid crystals indicate that ion diffusion is the charge transport mechanism that creates the space-charge field, a process that limits the efficiency and speed of the effect. The charge drift mechanism has not been a factor because of the short ionic drift length, L_E , given by

$$L_E = \frac{\mu^\pm \tau^\pm V}{d} \quad (3)$$

where τ^\pm is the carrier lifetime, V is the applied potential, and d is the cell thickness.¹⁴ Typically, $2\pi L_E \ll \Lambda$ in liquid crystals, while the drift mechanism can only contribute to a photorefractive grating if $2\pi L_E \geq \Lambda$.¹⁴

We now report on a photorefractive nematic liquid crystal composite containing the conjugated polymer poly(2,5-bis(2'-ethylhexyloxy)-1,4-phenylenevinylene), BEH-PPV that exhibits a novel fringe spacing depend-



ent inversion of the polarity of the space-charge field due to competition between the ionic diffusion and charge drift transport mechanisms. A eutectic mixture

* To whom correspondence should be addressed.

[†] Argonne National Laboratory.

[‡] Northwestern University.

(1) Moerner, W. E.; Silence, S. M.; Hache, F.; Bjorklund, G. C. *J. Opt. Soc. Am. B* **1994**, *11*, 320–30.

(2) Meerholz, K.; Volodin, B. L.; Sandalphon; Kippelen, B.; Peyghambarian, N. *Nature* **1994**, *371*, 497–500.

(3) Grunnet-Jepsen, A.; Thompson, C. L.; Twieg, R. J.; Moerner, W. E. *Appl. Phys. Lett.* **1997**, *70*, 1515–1517.

(4) Rudenko, E. V.; Sukhov, A. V. *JETP Lett.* **1994**, *59*, 142–46.

(5) Khoo, I. C.; Li, H.; Liang, Y. *Opt. Lett.* **1994**, *19*, 1723–25.

(6) Wiederrecht, G. P.; Yoon, B. A.; Wasielewski, M. R. *Science* **1995**, *270*, 1794–97.

(7) Wiederrecht, G. P.; Wasielewski, M. R. *J. Am. Chem. Soc.* **1998**, *120*, 3231–3236.

(8) Golemmé, A.; Volodin, B. L.; Kippelen, B.; Peyghambarian, N. *Opt. Lett.* **1997**, *22*, 1226–28.

(9) Ono, H.; Saito, I.; Kawatsuki, N. *Appl. Phys. Lett.* **1998**, *72*, 1942–44.

(10) Lundquist, P. M.; Wortmann, R.; Geletneky, C.; Twieg, R. J.; Jurich, M.; Lee, V. Y.; Moylan, C. R.; Burland, D. M. *Science* **1996**, *274*, 1182–85.

(11) Khoo, I. C.; Slussarenko, S.; Guenther, B. D.; Shih, M.-Y.; Chen, P.; Wood, W. V. *Opt. Lett.* **1998**, *23*, 253–255.

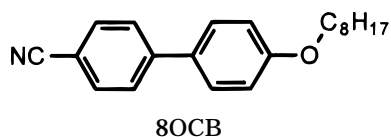
(12) Rudenko, E. V.; Sukhov, A. V. *JETP* **1994**, *78*, 875–882.

(13) Wang, Q.; Wang, L. M.; Yu, L. P. *J. Am. Chem. Soc.* **1998**, *120*, 12860–12868.

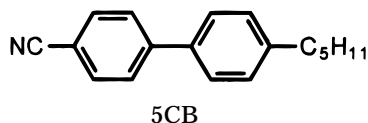
(14) Gunter, P. *Phys. Rep.* **1982**, *93*, 199–299.

(15) Maximus, B.; Ley, E. D.; Meyere, A. D.; Pauwels, H. *Ferroelectrics* **1991**, *121*, 103–112.

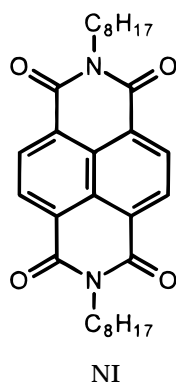
of 35% (wt %) 4'-(*n*-octyloxy)-4-cyanobiphenyl, 8OCB,



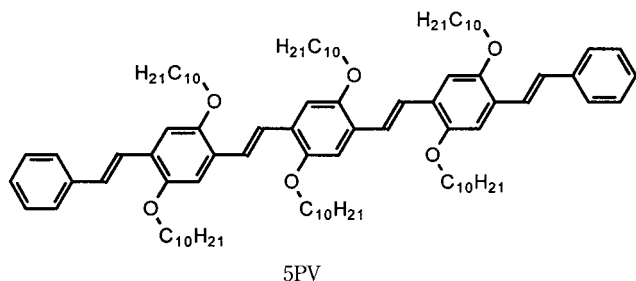
and 65% 4'-(*n*-pentyl)-4-cyanobiphenyl, 5CB, was doped



with 10^{-5} M BEH-PPV (200 kD by GPC), as the electron donor.¹⁶ The molecular weight of the BEH-PPV polymer implies that 500 repeat units of the monomer are present with an extended chain length of $0.35\ \mu\text{m}$. *N,N*-Diocetyl-1,4:5,8-naphthalenediimide, NI, 8×10^{-3} M, was



added as the electron acceptor.¹⁷ The free energy change for the photoinduced electron-transfer reaction, $1^* (\text{BEH-PPV}) + \text{NI} \rightarrow (\text{BEH-PPV})^+ + \text{NI}^-$, is $-1.0\ \text{eV}$.¹⁸ Two other liquid-crystal composites were also studied as controls. The first control composite contains the 5 unit phenylenevinylene oligomer, 5PV, as the electron donor



(4×10^{-5} M) along with the 8×10^{-3} M NI acceptor.¹⁹ The free energy change for the photoinduced electron-transfer reaction, $1^* 5\text{PV} + \text{NI} \rightarrow 5\text{PV}^+ + \text{NI}^-$, is -1.3

eV¹⁸ and is comparable to that for the BEH-PPV/NI pair. The second control composite contains 10^{-5} M BEH-PPV polymer with no NI present.

The liquid-crystal composites are sandwiched between two indium tin oxide coated glass slides that are functionalized with *n*-octadecylsilyl groups to induce homeotropic alignment.⁷ The cell thickness is $26\ \mu\text{m}$ as determined by a Teflon spacer. The concentrations of BEH-PPV and 5PV used in these experiments provide equal absorbances of $A = 0.02$ at 514 nm. A 1.5 V potential is applied to the cell to induce both directional charge transport and the orientational photorefractive effect.¹ All of the composites exhibit a dark conductivity of approximately $4 \times 10^{-11}\ \text{S}\cdot\text{cm}^{-1}$. The photoconductivities of the composites using 514 nm, $1\ \text{W}\cdot\text{cm}^{-2}$ irradiation are $1 \times 10^{-10}\ \text{S}\cdot\text{cm}^{-1}$ for both BEH-PPV/NI and 5PV/NI, and $3 \times 10^{-11}\ \text{S}\cdot\text{cm}^{-1}$ for the composite containing BEH-PPV alone.

Two coherent laser beams from an Ar⁺ laser with 1 mW total power at 514 nm and a beam diameter of 2.5 mm are overlapped in the sample to create an optical interference pattern.⁶ For these composites, asymmetric energy transfer (beam coupling) from one of the crossed laser beams to the other is observed. This phenomenon is characteristic for the photorefractive effect, wherein the refractive index grating is phase-shifted relative to the interference pattern.²⁰ Our experiments span the range of volume (Bragg) gratings at small Λ to thin (Raman-Nath) gratings at large Λ . In the thin-grating regime, other phenomena can also lead to the observation of asymmetric beam coupling, including thermal, photochromic, order-disorder, and phase change effects.²¹ However, these possibilities are ruled out using diagnostic experiments that have been discussed previously.^{7,12,22} For example, the direction of beam coupling reverses at all values of Λ , if the polarity of the applied static electric field is reversed. Additionally, the index grating is only observed for writing beams that are polarized with a component along x , consistent with an index change due to a modulated reorientation of the liquid-crystal director and not to absorption effects.²² As noted in other photorefractive studies in thin media, such as semiconductor quantum wells, the direction of beam coupling in both thin- and thick-grating regimes has the same dependence on the polarity of the space-charge field.²³

Figure 1a,b show the kinetics of beam coupling for two different values of Λ in the BEH-PPV/NI composite and the control composite containing 5PV/NI. With a comparison of the data illustrated in part a with those in part b of Figure 1, the direction of beam coupling at smaller Λ is the same for both composites, while it is opposite for the two composites at larger Λ . With a comparison of parts a and b in Figure 2 for $\Lambda < 5.5\ \mu\text{m}$, the direction of beam coupling in the BEH-PPV/NI composite is the same as that of the 5PV/NI control composite. Further observation reveals that beam coupling is observed in the BEH-PPV/NI composite at the

(16) Wang, B.; Wasielewski, M. R. *J. Am. Chem. Soc.* **1997**, *119*, 12–21.

(17) Greenfield, S. R.; Svec, W. A.; Gosztola, D.; Wasielewski, M. R. *J. Am. Chem. Soc.* **1996**, *118*, 6767–6777.

(18) The oxidation potentials, E_{OX} , of BEH-PPV and 5PV are both 0.9 V vs SCE, respectively, as determined by cyclic voltammetry. Their lowest excited-state energies, E_{S} , are 2.4 and 2.7 eV, respectively, as determined by the average of the energies of the lowest energy absorption band and highest energy band in their emission spectra. The reduction potential, E_{RED} , of NI is $-0.5\ \text{V}$ vs SCE. ΔG for photoinduced electron transfer is estimated as $E_{\text{OX}} - E_{\text{RED}} - E_{\text{S}}$.

(19) 5PV was prepared by a Wittig reaction of 2 mole of benzyltriphenylphosphonium bromide with the terminal dialdehyde of the corresponding 3-unit phenylenevinylene oligomer reported earlier.¹⁶

(20) Gunter, P.; Huignard, J. P. *Photorefractive Materials and Their Applications 1: Fundamental Phenomena*; Springer-Verlag: Berlin, 1988.

(21) Khoo, I. C. *Opt. Lett.* **1995**, *20*, 2137–39.

(22) Khoo, I. C. *IEEE J. Quantum Elec.* **1996**, *32*, 525–34.

(23) Wang, Q.; Brubaker, R. M.; Nolte, D. D.; Melloch, M. R. *J. Opt. Soc. Am. B* **1992**, *9*, 1626–41.

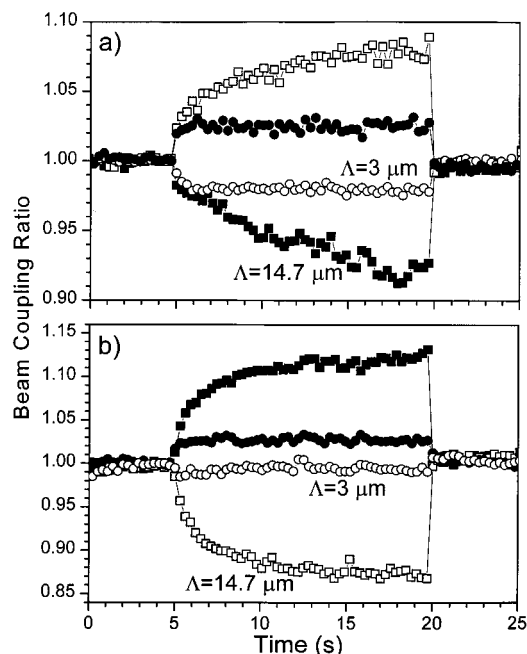


Figure 1. (a) The kinetics of beam coupling in the BEH-PPV/Ni liquid-crystal composite is shown for $\Lambda = 14.7 \mu\text{m}$ (\square and \blacksquare) and $3.0 \mu\text{m}$ (\circ and \bullet). (b) The kinetics of beam coupling in the 5PV/Ni liquid-crystal composite is shown for $\Lambda = 14.7 \mu\text{m}$ (\square and \blacksquare) and $3.0 \mu\text{m}$ (\circ and \bullet). The beam-coupling ratio for beam 1 is I_{12}/I_1 , where I_{12} is the intensity of beam 1, when both beam 1 and beam 2 are present in the sample, and I_1 is the intensity of beam 1 in the absence of beam 2. The corresponding beam-coupling ratio for beam 2 is I_{21}/I_2 , where I_{21} is the intensity of beam 2, when both beam 1 and beam 2 are present in the sample, and I_2 is the intensity of beam 2 in the absence of beam 1. Open symbols indicate the same beam, while solid symbols indicate the other beam. For each curve a photodiode monitors the intensity of one beam, while the other beam is incident on the sample at 5 s and blocked at 20 s.

high-resolution $\Lambda = 1.5 \mu\text{m}$,²⁴ whereas the smallest Λ achieved with the 5PV/Ni composite is $3 \mu\text{m}$. These observations are consistent with a space-charge field created through an ion diffusion mechanism. Within this model, the magnitude of the space-charge field in liquid crystals increases as the difference between the diffusion coefficients for the cation and anion increases.^{12,22} NI^- has a larger diffusion coefficient than oxidized electron donors of comparable size, including 5PV^+ .^{25,26} Since a BEH-PPV⁺ polymer cation has a much smaller diffusion coefficient than 5PV^+ , the space-charge fields derived from diffusion within both the BEH-PPV/Ni and 5PV/Ni composites should have the same polarity, and therefore, the same asymmetric energy exchange direction. The larger size and smaller diffusion coefficient of BEH-PPV⁺ relative to that of

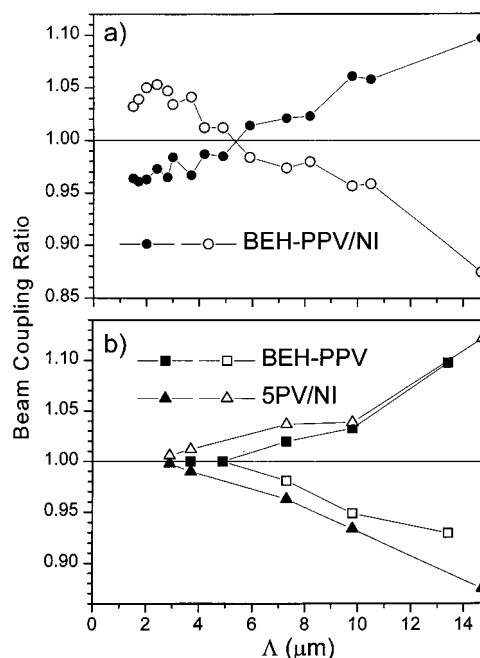


Figure 2. (a) The magnitude and direction of beam coupling in the BEH-PPV/Ni liquid-crystal composite is shown. (b) The beam-coupling ratio vs Λ for the control composites containing only BEH-PPV or 5PV/Ni is shown. Open symbols indicate the same beam for all three composites, while solid symbols indicate the other beam.

5PV^+ results in a higher resolution grating attained with the BEH-PPV/Ni composite because the difference in diffusion coefficients between BEH-PPV⁺ and NI^- is larger than that between 5PV^+ and NI^- .

The sign of the asymmetric beam coupling inverts for the BEH-PPV/Ni composite at approximately $\Lambda = 5.5 \mu\text{m}$, while neither control composite shows this inversion. This suggests that the polarity of the space-charge field inverts at this point.²⁰ With a comparison of parts a and b of Figure 2 for $\Lambda > 5.5 \mu\text{m}$, the direction of beam coupling in the BEH-PPV/Ni composite is the same as that with the control composite containing BEH-PPV alone. This indicates that the sign of the mobile charge carrier that contributes to space-charge field formation is the same for $\Lambda > 5.5 \mu\text{m}$ in these two composites, and opposite to that for the control composite containing 5PV/Ni. Therefore, since negative charges carried by diffusing NI^- are the most mobile charges that contribute to a phase-shifted space-charge field in the BEH-PPV/Ni composite for $\Lambda < 5.5 \mu\text{m}$, positive charges are the most mobile charges that contribute to a phase-shifted space-charge field at $\Lambda > 5.5 \mu\text{m}$.

Since the high 200 kD molecular weight of BEH-PPV⁺ precludes rapid ion diffusion, a charge migration mechanism other than diffusion is producing the space-charge field at larger values of Λ . Solutions of alkoxy-PPVs display very high intrachain mobilities for both holes and electrons.^{27,28} Fast hole transport along the BEH-PPV chain, coupled with hole hopping to other BEH-PPV chains, can lead to long distance hole migration in the composite. This mechanism of charge trans-

(24) The BEH-PPV/Ni composite at $\Lambda = 1.5 \mu\text{m}$ functions in the Bragg, thick-grating regime. Operating a photorefractive device in the Bragg regime is essential to carry out holographic information storage in these materials. The quality factor, Q , that determines whether the grating is in the Bragg diffraction regime is given as $Q = 2\pi D\lambda/\Lambda^2 n$, where D is the optical path length (for a tilt angle 30° relative to the homeotropic direction of the cell, $D = 26 \mu\text{m}/\cos 30^\circ = 30 \mu\text{m}$), λ is the wavelength, and n is the refractive index. $Q \gg 1$ is indicative of a Bragg regime grating. At $\Lambda = 1.5 \mu\text{m}$, $Q = 25$ and is comparable to typical Q values for photorefractive gratings in polymers, where $\Lambda \approx 3 \mu\text{m}$ and $D \approx 100 \mu\text{m}$.

(25) Wiederrecht, G. P.; Yoon, B. A.; Wasielewski, M. R. *Adv. Mater.* **1996**, *8*, 535–39.

(26) Wiederrecht, G. P.; Yoon, B. A.; Wasielewski, M. R. *Synth. Met.* **1997**, *84*, 901–2.

(27) Hoofman, R. J. O. M.; Haas, M. P. D.; Siebbeles, L. D. A.; Warman, J. M. *Nature* **1998**, *392*, 54–56.

(28) Davis, W. B.; Svec, W. A.; Ratner, M. A.; Wasielewski, M. R. *Nature* **1998**, *396*, 60–63.

port can be considered a charge drift mechanism in the trap density limited regime. This means that the charge drift length, L_E , is larger in the BEH-PPV-doped liquid crystals relative to the 5PV-doped liquid crystals. In the context of eq 3, it is likely that τ^\pm and μ^\pm are significantly enhanced in the BEH-PPV polymer due to the delocalization of charge and fast intrachain hole mobilities. The increase in τ^\pm and μ^\pm through this mechanism is not possible for smaller cations and anions such as 5PV⁺ and NI⁻. Furthermore, the magnitude of the current density due to drift should be larger (eq 2) in BEH-PPV-doped composites because n^\pm is proportional to the carrier lifetime.¹⁴ Thus, L_E and n^\pm are large enough in the BEH-PPV composite to observe charge drift as a contributor to space-charge field formation for the first time in liquid crystals.

The fringe-spacing limit in which each charge transport mechanism dominates is consistent with our analysis. The contribution to the magnitude of the space-charge field derived from ion diffusion is inversely proportional to Λ .^{12,22} However, the contribution to the space-charge field magnitude from charge drift, in the trap density limited model, is independent of Λ to a first approximation.¹⁴ The space-charge field due to drift can contribute to the photorefractive grating as long as $2\pi L_E \geq \Lambda$ so that the space-charge field is phase-shifted from the optical interference pattern. Therefore, in the BEH-PPV polymer/liquid-crystal composites where L_E is enhanced, the charge drift mechanism should dominate space-charge field formation at the larger values of Λ explored in our experiments, but the ion diffusion mechanism should dominate at smaller Λ (Figure 2). Furthermore, the fact that the control composite con-

taining only BEH-PPV does not show any beam coupling below 5.5 μm is consistent with the availability of only one charge transport mechanism, charge drift, because the absence of NI⁻ precludes diffusional space charge fields at lower values of Λ . This discussion only applies to which charge transport mechanism will dominate space-charge field formation at a given fringe spacing. The magnitude of the space-charge field does not correlate with the beam-coupling magnitude because the orientational response of liquid crystals decreases at smaller fringe spacings for $\Lambda < 2d$.²²

We have shown that the BEH-PPV conjugated polymer provides a mechanism to enhance the photorefractive effect in each fringe-spacing limit. In the ion diffusion limit, the much lower mobility of BEH-PPV⁺ relative to that of NI⁻ decreases the fringe spacing at which photorefractive beam coupling can be observed. Furthermore, the use of BEH-PPV enhances the charge drift length so that a new space-charge field generation mechanism in liquid crystals becomes possible. The versatility of conjugated polymers in enhancing the photorefractive effect in liquid-crystal composites may lead to the development of new optical devices that use photorefractivity for information processing and storage.

Acknowledgment. We gratefully acknowledge support from the Technology Research Division, Office of Advanced Scientific Computing Research, U.S. Department of Energy, under Contract W-31-109-ENG-38 (G.P.W.) and the Office of Naval Research under Grant N00014-99-1-0411 (M.R.W.).

CM9901008